Proceedings Paper:
Liu, S, Wang, J, Yu, HS et al. (2017) Numerical shakedown and non-shakedown responses of a Tresca half-space to a three-dimensional moving load. In: Proceedings. 19th International Conference on Soil Mechanics and Geotechnical Engineering (ICSMGE 2017), 17-22 Sep 2017, Seoul, Korea. ICSMGE, pp. 1385-1388.

Numerical shakedown and non-shakedown responses of a Tresca half-space to a three-dimensional moving load

Réponses numériques d'état limite et non-limite d'un demi-espace de Tresca à un ch argement en mouvement en trois dimensions

Shu Liu & Juan Wang
[1]Ningbo Nottingham New Materials Institute, The University of Nottingham, Ningbo, China; 199 Taikang East Road, Ningbo, 315100, China;
[2]State Key Laboratory for GeoMechanics and Deep Underground Engineering, China University of Mining & Technology, China, Shu.Liu@nottingham.edu.cn

Hai-Sui Yu & Dariusz Wanatowski
School of Civil Engineering, Faculty of Engineering, University of Leeds, Leeds, LS2 9JT, United Kingdom

ABSTRACT: Flexible pavements may fail due to excessive rutting as a result of accumulative plastic deformation; otherwise, if the load is small enough, pavements may deform plastically in the first number of load cycles and then reach a stable state which is termed as 'shakedown'. Recently some lower-bound and upper-bound solutions have been developed to directly determine the load limit (i.e. shakedown limit) below which an elastic-plastic half space can shake down. However, the actual responses of an elastic-plastic half-space subjected to repeated moving loads were not well revealed. In the present study, repeated moving surface loads are applied to a three-dimensional finite element model established in ABAQUS to research on the development of stresses and strains in a Tresca half-space. Also, a numerical shakedown limit can be determined according to the yield condition of structure under a static load following a number of load passes. It is found the development of residual stresses induced by plastic strains plays a key role in helping the half-space to reach the shakedown state. Good agreements are also observed between numerical and theoretical solutions for both shakedown limit and residual stress fields.

RÉSUMÉ: Les chaussées souples peuvent rompre à cause d'un orniérage excessif résultant de l'accumulation de déformations plastiques; mais si le chargement est assez petit, les chaussées peuvent se déformer de façon plastique au cours du premier nombre de cycles de chargement puis atteindre un état stable appelé 'état limite'. Récemment des solutions de limite inférieure et limite supérieure ont été développées pour déterminer directement le chargement limite (i.e état limite) sous lequel un demi-espace élasto-plastique peut s'établir. Cependant les réponses réelles d'un demi-espace élasto-plastique soumis à des chargements en mouvement répétés n'ont pas été correctement reproduites. Dans la présente étude, des chargements de surface en mouvement répétés sont appliqués à un modèle aux éléments finis tridimensionnel établi dans ABAQUS pour des recherches sur le développement de contraintes et déformations dans un demi-espace de Tresca. Une frontière numérique d'état limite peut être déterminée selon la condition de rupture de structure sous un chargement statique après un certain nombre de passages de chargement. Il a été montré que le développement de contraintes résiduelles induites par les déformations plastiques jouait un rôle clé favorisant le demi-espace à atteindre un état limite. Une bonne concordance entre les solutions numérique et théorique a été observée pour la frontière de l'état limite et les champs de contrainte résiduelle.

KEYWORDS: Shakedown; residual stresses; Tresca half-space; three-dimensional solutions

1 INTRODUCTION.

Shakedown theory can distinguish different long-term behaviours of elastic-plastic structures subjected to repeated or cyclic loads. According to Yu (2006), when the applied cyclic load is above the yield limit but lower than a critical load limit, termed as 'shakedown limit', the structure may exhibit some initial plastic deformation; however, after a number of load cycles, the structure may deform purely elastically without any further plastic deformation. This phenomenon is called 'shakedown'. Otherwise, if the load is higher than the shakedown limit, the structure will continue to exhibit plastic strains (known as ratchetting) for however long the load cycles are applied. In the field of pavement engineering, shakedown limit of a layered pavement system can be considered as a design load against unlimited increasing permanent deformation (excesssive rutting) under repaeated moving traffic load (Sharp and Booker 1984).

In the past few decades, theoretical solutions for shakedown limits of pavements were developed mainly based on two fundamental shakedown theorems (i.e. Melan's static shakedown theorem and Koiter's kinematic shakedown theorem). These two methods provide lower bound and upper bound to the true shakedown limit, respectively. This is because the static shakedown theorem satisfies the internal equilibrium equations and the stress boundary conditions, while the kinematic shakedown theorem satisfies the compatibility condition for plastic strain rate and boundary conditions for velocity. Upper bound shakedown solutions based on Koiter's kinematic shakedown theorem have been applied to two-dimensional (2D) and three-dimensional (3D) pavement problems (Collins and Cliffe 1987; Collins et al. 1993a,b; Ponter et al. 1985; Collins and Boulbibane 2000; Ponter and Engelhardt 2000; Boulbibane and Ponter 2005; Ponter et al. 2006; Li and Yu 2006). Besides, different methods based on Melan's static shakedown theorem were developed for Tresca or Mohr-Coulomb materials subjected to 2D and 3D repeated moving surface loads (e.g. Johnson 1962; Sharp and Booker 1984; Yu and Hossain 1998; Shiau and Yu 2000; Yu 2005; Krabbenhøft et al. 2007; Zhao et al. 2008; Wang 2011; Yu and Wang 2012; Wang and Yu 2013a,b, 2014; Liu et al. 2014, 2016). Yu and Wang (2012) solved the 3D lower bound shakedown solutions by introducing a critical self-equilibrated

residual stress field. However, the real repsonses of pavements to moving loads still needs to be researched.

In recent years, the development of computer technology has made it possible to conduct step-by-step numerical analyses. Wang and Yu (2013a) developed a numerical step-by-step approach to investigate the development of residual stress field in a cohesive-frictional half-space under two-dimensional repeated moving surface loads. Shakedown limit of such a structure can be determined according to the yield condition of structure under a static load following a number of load passes. In the present study, the numerical approach is extended to a 3D Tresca half-space to research on the development of stresses and strains after each load cycle in the 3D half-space. Also, comparisons are given between the numerical shakedown solutions and the theoretical shakedown solutions (Yu and Wang 2012).

2 PROBLEM DEFINITION

A 3D surface contact load limited within a circle of radius 'a' is considered, as shown in Figure 1. The pressure p on the contact surface is formulated as:

$$p = \frac{3P}{2\pi a^3}(a^2 - \mathrm{x}^2 - \mathrm{y}^2) \tag{1}$$

where P is the total normal load in the z-direction (i.e. the vertical direction). This load distribution is also known as the 3D Hertz load distribution. It has a maximum pressure $p_0 = 3P/2\pi a^2$ at the centre of the contact area.

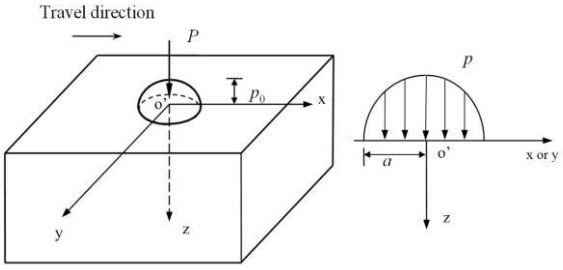

Figure 1. 3D Hertz pressure distribution.

3 NUMERICAL APPROACH

A semi-infinite body subjected to a quarter-spheral Hertz p ressure is considered in the present work to curtail the wo rking effort (Figure 2). Applictaion of the moving load is controlled by a user subroutine 'DLOAD'. The load is first applied gradually at the start point (A) and then moves incrementally on the pavement surface from A to B; this is to ensure the static equilibrium condition is fulfilled at each time increment during the entire loading history. Two-loading areas are located at the two sides of the model to eliminate the effects of boundary conditions. At the end of each load pass, the applied load is removed thoroughly to investigate stresses remaining in the pavement (i.e. residual stress). After a few load passes, a static load with same magnitude of the moving load is applied in the middle on the pavement surface. If no yielding point can be found in the pavement (i.e. the total stress state of each point in the pavement does not violate the yield criterion), a steady state (termed as 'shakedown state') is achieved. In contrast, any yielding point would indicate that the applied load is above the shakedown limit of the pavement and the whole structure is in a non-shakedown state. Several numerical simulations with different load magnitudes are performed to determine the shakedown limit.

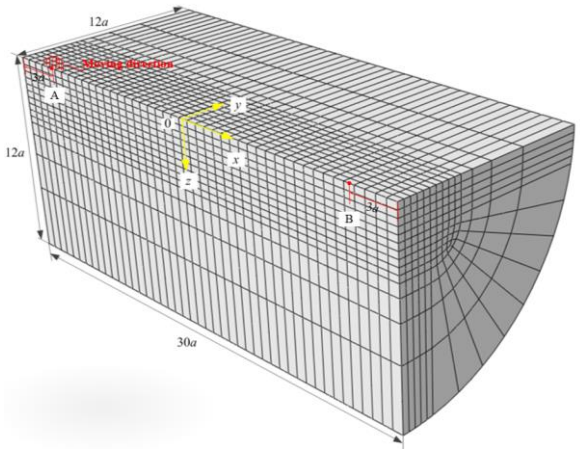

Figure 2. 3D model sketch and FE model.

4 MODEL DESCRIPTION AND VERIFICATION

A 3D model was established in the finite element software ABAQUS as shown in Figure 2.The dimension of the 3D model is smaller than the one used in 2D numerical shakedown analyses (Liu et al. 2016) because of the relatively small affected area. Symmetric boundary conditions are applied on the plane of $y = 0$. Both vertical (i.e. z direction) movement and horizontal movement in the x direction are constrained on the cambered surface. Constraints on horizontal movements of the two sides are also applied. The element type is selected as C3D20R, which stands for Continuum, 3D, 20 noded reduced integrated elements. Table 1 shows different mesh densities used for sensitivity study and the corresponding results. The shakedown limits decrease with increasing mesh density. In the following study, the mesh with 7695 elements is used (Figure 3). It can be found that its 3D numerical shakedown limits are close to the theoretical solution of Yu and Wang (2012).

Table 1. Influence of mesh density on 3D numerical shakedown limits.

Model	Number of Elements	Theoretical shakedown limit (Ref)	Numerical shakedown limit	Average elapsed time per load pass (hr)
1	1920		5.3c	0.05
2	4320	4.68c	4.5c	0.78
3	7695		4.5c	2.21

5 SOLUTIONS AND DISCUSSIONS

Tresca material is considered in the present study. By using the numerical approach, some yielding areas are observed under a static load following four load passes ($p_0 = 4.6c$) (Figure 3). It is also demonstrated that the yielding area initiate on the plane y = 0, which is consistent with the theoretical findings of Yu and Wang (2012).

Wang and Yu (2013a) indicated that the residual stresses in 2D half-space under moving surface load barely change after several load passes. In the present study, this phenomnon is also observed for the 3D problem after three load passes. As everywhere along the load moving direction experiences the same loading history, the residual stresses should be independent of the travel dirction. Figure 4 shows an example for the fully-developed horizontal residual stress (σ_{xx}^r) in the central plane.

As mentioned by Wang and Yu (2013a), σ_{xx}^r and σ_{yy}^r exist in 2D problems; however, all six residual stress components could exist in 3D problems. On any x-z plane, σ_{zz}^r, σ_{xy}^r, σ_{xz}^r

and σ_{yz}^r are very small compared with σ_{xx}^r and σ_{yy}^r (Figure 5). This agrees with Kulkarni et al. (1990) and Jiang et al. (2002)'s findings, in which the stress analyses were carried out on 3D rolling contact problems with Von-Mises materials. Figure 5 also indicates that σ_{xx}^r and σ_{yy}^r on all the planes normal to the y-axis attain their peak values at a depth of z = 0.4*a*. This agrees with Wang (2001)'s theoretical finding of z = 0.36*a*. The residual stress field is almost zero when $z \leq 1.2a$. In addition, the values of σ_{xx}^r and σ_{yy}^r are largest at the plane of y = 0. Figure 6 also demonstrates that σ_{yy}^r can be treated as the intermediate residual stress on the plane of y = 0.

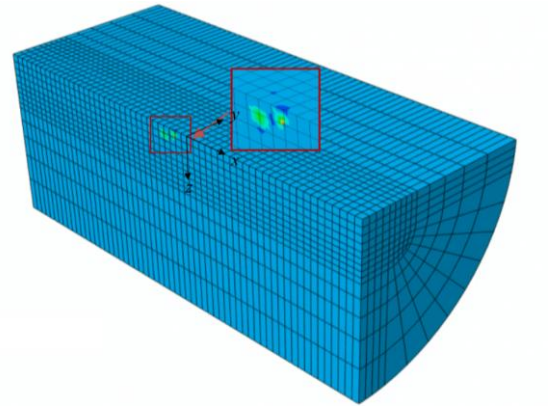

Figure 3. Location of yielding areas in a 3D model.

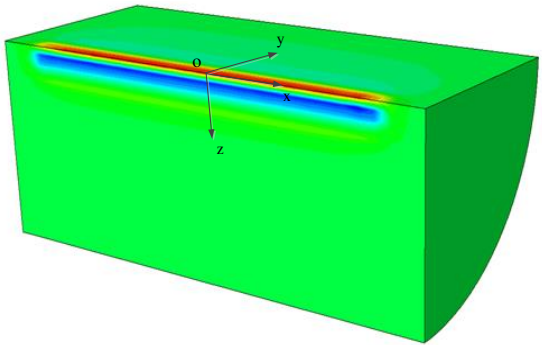

Figure 4. Distributions of the residual stresses after four load passes.

According to Yu and Wang (2012), the real residual stress should be contained by two crtical resiudal stress fields. Comparisons are made between the horizontal residual stresses obtained by the numerical approach and the critical residual stresses calculated by the their theoretical approach (Figure 7). When p_0 = 4.6c, the FE calculated residual stress field deviates from the critical residual stresses at around z = 0.4*a* (refer to Figure 7), which means the load applied is larger than the numerical shakedown limit. When the applied load is decreased to 4.5c (i.e. the numerical shakedown limit), the FE calculated residual stresses are bracketed by the critical residual stress fields.

All the six components of strain are non-zero for the 3D analysis. The locations of the most critical depths of normal plastic strain are consistent with those of the normal stress, i.e. z = 0.45*a*. ε_{yy}^p is higher than ε_{xx}^p due to less constraints in the y direction. Since every point in the horizontal direction experiences the same loading history, the generation of the plastic strains in the horizontal direction is also related to the shear strains in x-z planes and x-y planes. In terms of the plastic normal strain ε_{yy}^p, it was zero in the 2D analysis as the plane strain assumption was made, but becomes tensile in the 3D analysis. The most significant normal strain is observed in the vertical direction, and the integration of the vertical strain over the depth indicates the vertical deformation on the surface, i.e. rutting. From Figure 8, shear strains ε_{xz}^p are more significant than ε_{yz}^p and ε_{xy}^p. The negative and positive values of ε_{xz}^p demonstrate forward and backward shear flows respectively at different depths in the pavement. The shear strains ε_{xy}^p are related to different amounts of shear flows at the same depth in the transverse direction. The shear strains ε_{yz}^p are attributed to different vertical deformations at the same depth in the transverse direction.

In summary, the response of pavement foundation under repeated moving traffic load can be observed through the numerical step-by-step approach. A new pavement design load against excessive rutting (i.e. shakedown limit) can also be obtained by examining the yield condition of the structure under a static load after a few number of load passes. It is worth noting that the numerical step-by-step approach can be easily implemented to more realistic problems. For instance, the pavement structure can be considered as a layered system and the material plastic responses can be described by more complicated constitutive models. Furthermore, this approach can also be used to simulate the roller compaction process on the pavement foundation; thereby predicting the required number of load passes when a certain magnitude of moving load is applied.

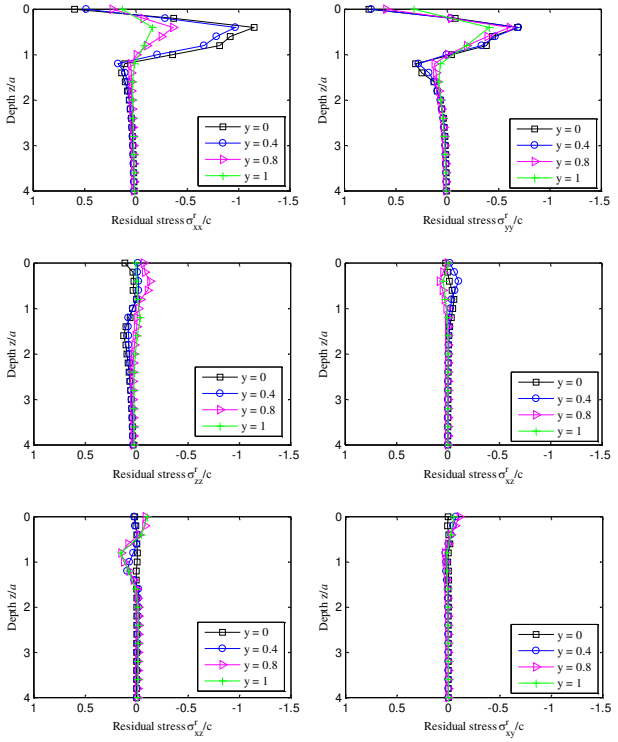

Figure 5. Residual stresses after four load passes.

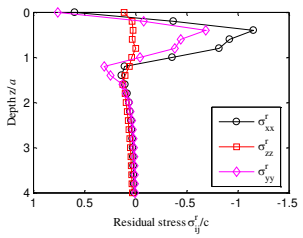

Figure 6. Residual stress fields after four load passes when p_0 = 4.5c when y = 0.

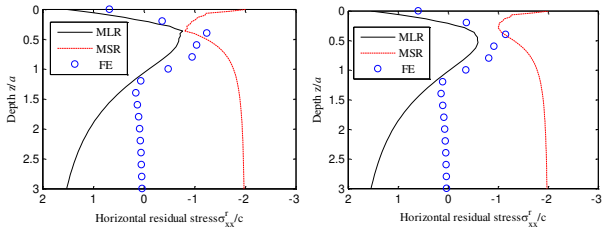

(a) $p_0 = 4.6c$ (b) $p_0 = 4.5c$

Figure 7. Development of horizontal residual stress σ_{xx}^{r} under successive load passes.

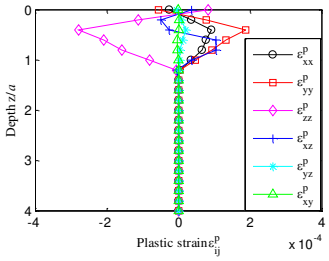

Figure 8. Plastic strain fields at $y = 0$ after four load passes when $p_0 = 4.5c$.

6 CONCLUSIONS

In this paper, a numerical step-by-step approach was applied to a 3D Tresca half-space to obtain the shakedown limit and investige the distributions of residual stresses and plastic strains. It is found that the plane of y = 0 is the most critical plane; this is consistent with the theoretical findings of Yu and Wang (2012). Good agreements are also shown between the numerical and theoretical 3D shakedown limits. The fully-developed residual stress field obtained from the numarical approach is bounded by two critical residual stress fields when the structure is in shakedown state. Further study will be carried out by considering the Mohr-Coulomb materials.

7 ACKNOWLEDGEMENTS

Financial supports from National Natural Science Foundation of China (Grant No. 51408326) is gratefully acknowledged.

8 REFERENCES

Boulbibane M. and Ponter A.R.S. 2005. Linear Matching Method for Limit Load Problems Using the Drucker-Prager Yield Condition. *Géotechnique*, 55, 731-739.

Collins I.F. and Cliffe P.F. 1987. Shakedown in Frictional Materials under Moving Surface Loads. *International Journal for Numerical and Analytical Methods in Geomechanics*, 11 (4), 409-420.

Collins I.F., Wang A.P. and Saunders L.R. 1993a. Shakedown in Layered Pavements under Moving Surface Loads. *International Journal for Numerical and Analytical Methods in Geomechanics,* 17 (3), 165-174.

Collins I.F., Wang A.P. and Saunders L.R. 1993b. Shakedown Theory and the Design of Unbound Pavements. *Road and Transport Research,* 2 (4), 28-39.

Collins I.F. and Boulbibane M. 2000. Geomechanical Analysis of Unbound Pavements Based on Shakedown Theory. *Journal of Geotechnical and Geoenvironmental Engineering*, 126 (1), 50-59.

Johnson K.L. 1962. A Shakedown Limit in Rolling Contact. *Procedings of the 4th US National Congress of Applied Mechanics*, Berkeley, California, 971-975.

Koiter W.T. 1960. General Theorems for Elastic-Plastic Solids. *In Progress in Solid Mechanics, edited by R. Hill. eds I. N. Sneddon. North-Holland*, Amsterdam.

Krabbenhøft K., Lyamin A.V. and Sloan S.W. 2007. Shakedown of a Cohesive-Frictional Half-Space Subjected to Rolling and Sliding Contact. *International Journal of Solids and Structures*, 44 (11–12), 3998-4008.

Li H.X. and Yu H.S. 2006. A Nonlinear Programming Approach to Kinematic Shakedown Analysis of Frictional Materials. *International Journal of Solids and Structures*, 43 (21), 6594-6614.

Liu S., Wang J., Yu H.S. and Wanatowski D. 2014. Shakedown of Layered Pavements under Repeated Moving Loads. *Geo-Shanghai 2014*. Shanghai, 179-188.

Liu S., Wang J., Yu H.S. and Wanatowski D. 2016. Shakedown Solutions for Pavements with Materials following Associated and Non-associated Plastic Flow Rules. *Computers and Geotechnics*, 78, 218-266

Melan E. 1938. Der Spannungsgudstand Eines Henky-Mises Schen Kontinuums Bei Verlandicher Belastung. *Sitzungberichte der Ak Wissenschaften Wie*, 147 (73).

Ponter A.R.S., Hearle A.D. and Johnson K.L. 1985. Application of the Kinematical Shakedown Theorem to Rolling and Sliding Point Contacts. *Journal of the Mechanics and Physics of Solids*, 33 (4), 339-362.

Ponter A.R.S. and Engelhardt M. 2000. Shakedown Limits for a General Yield Condition: Implementation and Application for a Von Mises Yield Condition. *European Journal of Mechanics A/Solids*, 19 (3), 423-445.

Ponter A.R.S., Chen H.F., Ciavarella M. and Specchia G. 2006. Shakedown Analyses for Rolling and Sliding Contact Problems. *International Journal of Solids and Structures*, 43 (14–15), 4201-4219.

Sharp R.W. and Booker J.R. 1984. Shakedown of Pavements under Moving Surface Loads. *Journal of Transportation Engineering*, ASCE, 110, 1-14.

Shiau S.H. and Yu H.S. 2000. Load and Displacement Prediction for Shakedown Analysis of Layered Pavements. *Transportation Research Record: Journal of the Transportation Research Board* 1730 (1), 117-124.

Wang J. 2011. Shakedown Analysis and Design of Flexible Road Pavements under Moving Surface Loads, Ph.D. thesis, The University of Nottingham, UK.

Wang J. and Yu H.S. 2013a. Residual Stresses and Shakedown in Cohesive-Frictional Half-Space under Moving Surface Loads. *Geomechanics and Geoengineering*, 8 (1), 1-14.

Wang J. and Yu H.S. 2013b. Shakedown Analysis and Design of Layered Road Pavements under Three-dimensional Moving Surface Loads. *Road Materials and Pavements Design*, 14, 703-722.

Wang J. and Yu H.S. 2014. Three-dimensional Shakedown Solutions for Anisotropic Cohesive-Frictional Materials under Moving Surface Loads. *International Journal for Numerical and Analytical Methods in Geomechanics*, 38 (4), 331-348.

Yu H.S. and Hossain M.Z. 1998. Lower Bound Shakedown Analysis of Layered Pavements Using Discontinuous Stress Fields. Computer *Methods in Applied Mechanics and Engineering*, 167 (3-4), 209-222.

Yu H.S. 2005. Three-Dimensional Analytical Solutions for Shakedown of Cohesive-Frictional Materials under Moving Surface Loads. *Proceedings of the Royal Society A: Mathematical, Physical and Engineering Science,* 461 (2059), 1951-1964.

Yu H.S. 2006. *Plasticity and Geotechnics.* Springer, UK.

Yu H.S. and Wang J. 2012. Three-Dimensional Shakedown Solutions for Cohesive-Frictional Materials under Moving Surface Loads. *International Journal of Solids and Structures*, 49 (26), 3797-3807.

Zhao J., Sloan S.W., Lyamin A.V. and Krabbenhøft K. 2008. Bounds for Shakedown of Cohesive-Frictional Materials under Moving Surface Loads. *International Journal of Solids and Structures*, 45 (11-12), 3290-3312.